

Surfactant Adsorption at Solid–Aqueous Interfaces Containing Fixed Charges: Experiments Revealing the Role of Surface Charge Density and Surface Charge Regulation

Aysen Tulpar and William A. Ducker*

Virginia Polytechnic Institute and State University, Blacksburg, Virginia 24061

Received: March 25, 2003; In Final Form: November 11, 2003

The charge on the solid–liquid interface affects both the amount of ionic surfactant and the organization of the surfactant adsorbed at the solid–liquid interface. For most solids, the surface charge is not fixed; it is regulated by the adsorption or desorption of ions. The aim of this work is to study surfactant adsorption to surfaces that have a *controlled* and *fixed* density of covalently bound surface charges. The desired surface charge density is achieved by the use of gold–thiol self-assembled monolayers (SAMs) of different ω -groups ($-\text{OH}$ and $-\text{N}^+(\text{CH}_3)_3$). The mole fraction of $-\text{N}^+(\text{CH}_3)_3$ on the mixed SAM dictates the density of covalently bound charges. The charge on $-\text{N}^+(\text{CH}_3)_3$ is fixed and does not self-regulate, but the total surface charge can be changed through adsorption of other ions. We have studied the adsorption of sodium dodecyl sulfate (SDS) to the interface between these model surfaces and aqueous solutions of SDS. Atomic force microscopy (AFM) of the adsorbed surfactant reveals no surface micelles above the critical micelle concentration, cmc, over a wide variety of $-\text{N}^+(\text{CH}_3)_3$ densities. This leads us to hypothesize that lateral mobility of ions other than surfactant at the interface is important for the formation of surface micelles of ionic surfactants. Adsorption isotherms of SDS (with no added salt) measured by surface plasmon resonance (SPR) show a plateau region that ends at about $\text{cmc}/25$. In this plateau region, the surface excess of SDS is equal to the known fixed surface charge. There is a second plateau region above the cmc. In this concentration range, the surface excess is approximately twice the fixed surface charge. Desorption experiments starting above the cmc show rapid desorption of SDS into water until the surface excess is equal to the fixed surface charge. The rapid desorption is followed by a much slower desorption.

Introduction

Surfactant adsorption is widely used to achieve changes in wetting, colloidal properties, and lubrication. Many surfactants are charged, and it is well-known that the charge on the solid–liquid interface affects the amount of adsorption, the shape of the adsorption isotherm,^{1–3} and the organization of the adsorbed surfactant molecules.⁴ The adsorption of cationic surfactants to solid–aqueous interfaces has recently been reviewed.⁵ However, to date there has not been a study of the adsorption of surfactants in which the magnitude and or the distribution of surface charges has been controlled independently of the surfactant adsorption. The reason is that for most solid–liquid interfaces the interfacial charge is not fixed but is regulated by adsorption and desorption of ions, including the surfactant ions. For example, the surface charge of silica is regulated by adsorption of H^+ ions⁶ and by adsorption of quaternary ammonium surfactants.⁷ In this paper we describe the fabrication of solid–aqueous interfaces with a controlled and fixed density of surface charges that are covalently bound to the solid, and we describe the adsorption of the surfactant, sodium dodecyl sulfate (SDS), to these interfaces.

Unfortunately, there is no universally accepted definition of surface charge. This is a consequence of the finite width of the interface and our difficulty in directly probing the structure of the interface. On some occasions the term “surface charge” is used to describe the charge developed either by dissociation of groups covalently bound to the solid² or dissolution of lattice

ions, and on other occasions it is obtained from fits to surface force or from electrophoretic measurements. The latter evaluate electrostatic properties at a plane further from the bulk solid, and so ions that are not directly bound to the solid are included in the surface charge. Examples of the former are hydrogen ions adsorbed to silica, and examples of the latter are hydrated sodium ions adsorbed to silica. It is not always possible to categorize adsorption into one or the other of these categories. In this paper we describe adsorption to surfaces with a controlled and fixed amount of charge that is covalently bound to the solid, so we sidestep the difficulties in describing the position of the surface charge and simply use the symbol σ_c to represent the covalently bound charge per unit area. For brevity, we refer to this as the surface charge density. We will use the term “outer surface charge” to describe the charge in the plane separating the diffuse double-layer from more strongly held adsorbates. The outer surface charge is equal to minus the diffuse layer charge, $-\sigma_D$, (see Figure 1) and is necessarily a vague term because not all details of the interfacial structure are known.

Charge regulation is of fundamental importance to the adsorption of ionic surfactants because it allows surfactant adsorption to increase without a stoichiometric change in the outer surface charge.⁷ A stoichiometric change in the outer surface charge inhibits the adsorption of like-charged surfactant by raising an electrostatic barrier to adsorption. Charge regulation can occur both at the solid surface directly (e.g., on silica, by dissociation of a silanol group) and in the thin film adjacent to the surface (outer-charge regulation) through the adsorption of surfactant, surfactant counterions, and other salts.

* To whom correspondence should be addressed. E-mail: wducker@vt.edu.

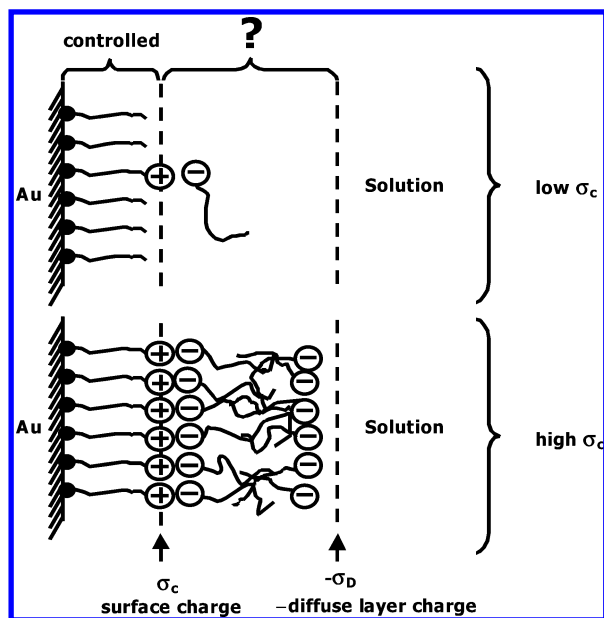


Figure 1. Model for surface charge density and surfactant adsorption. The black spheres, the positively charged headgroups, and the negatively charged headgroups represent $-S$, $-N^+(CH_3)_3$, and $-OSO_3^-$, respectively.

Charge regulation is very important in the adsorption of charged surfactants. For example, at low surfactant concentrations the adsorption of sodium dodecyl sulfate to alumina increases while the zeta potential is approximately constant.⁸ This suggests that the (positive) surface charge of the alumina increases to compensate for the increase in the negative charge caused by the surfactant adsorption. Work by Koopal and co-workers on silica has revealed charge regulation by the measurement of H^+ ions that are released from silica during the adsorption of quaternary alkylammonium and pyridinium surfactants.⁷ On silica, the maximum surface charge regulation occurs at low salt and surfactant concentrations. At low salt and surfactant concentrations, approximately one proton desorbs for every two surfactant molecules that adsorb, and when the outer surface charge is zero, approximately one proton desorbs for every additional surfactant molecule that adsorbs. Koopal and co-workers have also studied the effect of salt concentration on adsorption. They find a “common intersection point” (cip) where adsorption isotherms at different salt concentrations approximately intersect and the outer charge on the surface is approximately zero. Goloub and Koopal⁹ explain this phenomenon by suggesting that salt hinders adsorption below the cip when electrostatic interactions between the silica and the surfactant promote adsorption and salt promotes adsorption above the cip when electrostatic interactions among surfactant molecules hinder adsorption. At higher surfactant concentrations the outer surface charge is strongly regulated by the adsorption of surfactant counterions.¹⁰

Surfactant adsorption is also controlled by forces acting on the hydrophobic tail. There is often a concentration range where the surface excess of surfactant increases rapidly with concentration. This is known as the hemimicelle concentration,¹¹ and there is evidence to support the idea that the acceleration in adsorption is due to a decrease in the amount of water in contact with the alkyl chains. The energy decrease through partial or full removal of the alkyl chain from the aqueous environment (~ 1 kT per methylene group¹²) is often enough to overcome the energy penalty of charging the surface.

One critical role of charge regulation is therefore to suppress the electrostatic penalty for adsorption until the surfactant density

is high enough to allow many lateral interactions between the surfactant tails. This enables hemimicelle formation at low concentrations. Implicit in most ideas of charge regulation is the idea that charges are free to migrate across the surface. Thus, a charge-regulating surface facilitates adsorption of a cluster of surfactant molecules through the creation of a cluster of surface charges on *neighboring* surface sites. In a recent review, Atkin et al.⁵ suggest that the adsorption of charged surfactant to silica should enhance adsorption of surfactant to neighboring sites by increasing the acidity of neighboring silanol groups.

In this paper we further understanding of the role of charge regulation in the adsorption of ionic surfactants by controlling one component of the surface charge: the density of charged groups that are covalently bound to the solid. We create these fixed-charge surfaces by adsorption to gold of mixed self-assembled monolayers (SAMs)¹³ of ω -functionalized thiols from solution. The monolayer components are $S(CH_2)_{11}OH$, which we abbreviate as ω -OH, and $S(CH_2)_{11}N^+(CH_3)_3$, which we abbreviate as ω -TMA. The surface density of ω -TMA can be changed during the deposition of the thiol monolayer by altering the concentration of $HS(CH_2)_{11}N^+(CH_3)_3Cl^-$ in the deposition solution. We are not able to control or measure the distribution of ω -TMA on the surface, but we assume that Coulombic repulsion during film formation prevents the formation of clusters of charge. We also assume that ω -TMA and ω -OH do not reorganize in the SAM during surfactant adsorption because of the strong sulfur–gold bonds between the thiolate and the gold.¹⁴ The water wettability is approximately constant over the composition range from 0% to 100% ω -TMA (see the results section), so we are able to change the surface charge density while maintaining almost constant wettability.

Each ω -TMA contains one fixed positive charge, so σ_c is dictated by the density of ω -TMA on the surface:

$$\sigma_c = e \alpha \Gamma_{SAM} \quad (1)$$

where e is the magnitude of the charge on an electron, α is the surface mole fraction of ω -TMA in the SAM, and Γ_{SAM} is the number of molecules per unit area in the SAM.

The outer surface charge can be regulated by adsorption of ions from solution. We have not used any buffers or extraneous ions, so free ions only arise from the surfactant (SDS), the initial counterions to the TMA (Cl^-), the dissociation of water, and the hydration of CO_2 . SDS is a strong electrolyte, so the DS^- concentration is stoichiometric to the added SDS up to the critical micelle concentration (cmc). The OH^- , CO_3^{2-} , and HCO_3^- concentrations can be calculated from the pH and the carbonate dissociation constants. These concentrations are approximately 10^{-8} M, 10^{-11} M, and 10^{-6} M, respectively; all are much smaller than the DS^- concentration. The very few Cl^- ions will be washed out in the initial rinse with water. From earlier experiments¹⁵ we have indirect evidence that suggests that the OH^- , CO_3^{2-} , and HCO_3^- ions have no particular affinity for the $-N^+(CH_3)_3$ group, so we will assume that DS^- is the only significant counterion. Likewise, the most abundant co-ion is the Na^+ produced by dissociation of SDS. So, to a good approximation the only outer charge regulation occurs through adsorption of the surfactant (Na^+ and DS^-). We also report on the results of an experiment in which additional outer charge regulation is introduced by adding NaCl into solution. Studies of ion binding to quaternary ammonium surfactants show that there is a nonionic contribution to the binding of halides to the $-N^+(CH_3)_3$ group.¹⁶

In summary, we are able to produce interfaces in which the average covalently bound surface charge density is controlled,

known, and fixed in magnitude and the position of each surface charge is fixed to the end of an alkyl chain. Thus, we can study surfactant adsorption to highly controlled surfaces where outer charge regulation is limited to adsorption of the surfactant, and we can introduce further charge regulation by the addition of salt.

Experimental Section

Materials. SDS (Sigma, St. Louis, MO) was recrystallized twice from 200-proof ethanol (Aaper Alcohol Chemical Co., USA). The concentration of surface-active contaminants was low as shown by the fact that surface tension measurements revealed no minimum in the surface tension versus $\ln(\text{concentration})$ curves. Solutions were prepared with 18.3 MW deionized, charcoal-filtered water (EASYpure UV, Barnstead Thermolyne Corp., Dubuque, IA). SDS solutions were used within 1 h of preparation from the solid to prevent formation of dodecanol. KOH (Aldrich, Milwaukee, WI) was semiconductor grade and was used as received. NaCl (Sigma, St. Louis, MO) was roasted in air at 400 °C for 16 h. 11-Mercapto-1-undecanol (Aldrich, Milwaukee, WI), 97%, was used as received.

N,N,N-Trimethyl(11-mercaptoundecyl)ammonium chloride was synthesized according to the procedure in ref 17. It was recrystallized from *tert*-butyl methyl ether and ethanol (90:10). NMR (D_2O , δ): 1.24–1.49 (m, 14 H, CH_2), 1.53–1.66 (m, 2 H, $\text{CH}_2\text{CH}_2\text{SH}$), 1.67–1.84 (m, 2 H, $\text{CH}_2\text{CH}_2\text{NMe}_3^+$), 2.52 (t, 8 H, 2 H, CH_2SH), 3.12 (s, 9 H, NMe_3^+), 3.30–3.41 (m, 2 H, $\text{CH}_2\text{NMe}_3^+$). MS (FAB): 246 (100%). MS (high-resolution): 246.2259.

Atomic Force Microscopy (AFM). Images were captured in situ using a Nanoscope III AFM (Digital Instruments, CA) using silicon cantilevers (Park Scientific, CA) with nominal spring constants of 0.26 N/m. Before each experiment, the cantilevers were irradiated for at least 30 min in a laminar flow cabinet with ultraviolet light ($\sim 9 \text{ mW/cm}^2$ at 253.7 nm) generated from a PENRAY Lamp (UVP, Inc., Upland, CA). The solution was held in a fluid cell and sealed by a silicone O-ring. Prior to use, the fluid cell and the O-ring were soaked in SDS solution, rinsed with water, and dried with high-purity N_2 . The z -axis of the piezo was calibrated by a silicon calibration reference of 22.0 nm step height (Silicon-MDT, Moscow, Russia). The x - and y -axes of the piezo were calibrated by imaging a diffraction grating replica of 2160 lines/mm waffle pattern (Ted Pella, Redding, CA).

Measurements were performed in the temperature range of 22 ± 2 °C, at pH 6, and at 16 mM SDS. The integral and proportional gains were in the range of 0.1–0.6, and scan rates were in the range of 3–6 Hz. All images reported here are unfiltered deflection images. Images were captured at the maximum force that would allow stable imaging before the characteristic instability that is associated with displacement of the surfactant film.

The gold samples for AFM measurements were fabricated from a 1 cm long, 1 mm diameter 99.99% gold wire (Alfa Aesar, Ward Hill, MA). The Au wire was cleaned in piranha solution (7:3 concentrated H_2SO_4 /30% H_2O_2), rinsed with water, and left in ethanol. After removing the Au wire from ethanol, one end of the Au wire was heated in a H_2/O_2 flame until it was red hot and molten. The end of the wire was approximately spherical (~ 2 –3 mm diameter) and contained about two small flat facets.^{18–20} When the Au ball was annealed in a cooler region of the H_2/O_2 flame, the size of each Au (111) facet was increased, and it was readily observed with an optical microscope.²¹ Immediately after the removal of the Au wire from

the H_2/O_2 flame, the gold ball was immersed in a 2 mM solution of the thiol (mixture) in chloroform (HPLC grade) and was left immersed for 24–48 h. Before the AFM experiment, the Au wire was sonicated for 5 min in chloroform to remove the physisorbed molecules and leave only molecules that are bound by strong gold–sulfur bonds. The Au ball was oriented in a home-built specimen holder to expose a facet for AFM measurements.

Surface Plasmon Resonance (SPR). SPR data were obtained using a Reichardt Bio-SPR 9000 instrument (Reichardt Inc., Depew, NY). This system uses a 10-W tungsten halogen lamp with filters for p-polarized 760 nm light. The substrates for SAMs were 1 cm^2 glass slides coated with 10 Å of chromium and 40 nm of gold (Reichardt Inc.). The gold-plated glass slides were optically coupled to the prism using a high refractive index liquid, 1.5150 (Cargille, Cedar Grove, NJ). The flow cell surface area was 11 mm \times 4 mm. The flow cell volume was 5 μL . Prior to each experiment, the fluidics of the SPR instrument was rinsed with purified water for 2 h. SDS solutions were analyzed after the SAM substrate was put into the cell and a steady baseline was established in water. The concentration range for SDS solutions was 0.02–33 mM. Each solution was run for 5 min. Between measurements of different SDS solutions, the cell was rinsed with water for 5 min.

All gold-on-glass substrates for the SPR experiments were cleaned in freshly prepared piranha solution for 1 min and then rinsed with water, ethanol, and chloroform. SAMs were prepared by 24–48 h exposure of the gold substrates to 2 mM solutions of the thiols in chloroform (HPLC grade) in single-use scintillation vials (20 mL). The slides were removed from the solutions, washed with chloroform and ethanol, and dried with N_2 prior to the experiments. Measurements were recorded at 22 ± 2 °C.

X-ray Photoelectron Spectroscopy (XPS). Spectra were obtained using a Perkin-Elmer PHI 5400 model X-ray photoelectron spectrometer with an Mg K α achromatic X-ray source (1253.6 eV), operating at 14 keV and 400 W. The chamber pressure was $\sim 1 \times 10^{-8}$ Pa, and the takeoff angle (measured as the angle between the sample normal and the photoelectron analyzer) was 15°. Each sample was examined with both a survey scan, encompassing the region 0–1100 eV, and a multiplex scan of carbon, oxygen, sulfur, gold, and nitrogen. Binding energies of all photopeaks were referenced to the C1s photopeak position for C–C and C–H species at 285 eV. The X-ray anode was adjusted to 1246.6 eV to bring the C1s peak to 285 eV. The photopeaks were analyzed by subtracting the X-ray source line width and determining the number of counts for each peak on an Apollo 3500 computer, using PHI software, version 4.0. For each photopeak this analysis was carried out 10 times. The average value, with appropriate sensitivity factors, was used to calculate the peak areas. The error in peak areas was determined from the standard deviation.

Slides of 4 cm^2 glass–gold substrates (Evaporated Metals Inc., Ithaca, NY) were used for the XPS experiments. One slide was cut into four squares so as to keep the Au layer the same. This was necessary because the photopeak area ratios of S and Au depended on the thickness of Au on the glass. SAMs of ω -OH, ω -TMA, and mixed SAMs (0.25 and 0.5 mole fractions of $\text{HS}(\text{CH}_2)_{11}\text{N}(\text{CH}_3)_3\text{Cl}$ in solution) were prepared from these four slides.

Cyclic Voltammetry. Experiments were performed in a three-electrode cell with an electrochemical analyzer (CH Instruments, TN). The working electrode was a Au (111) single crystal (Evaporated Metals Inc., Ithaca, NY), and the exposed area was

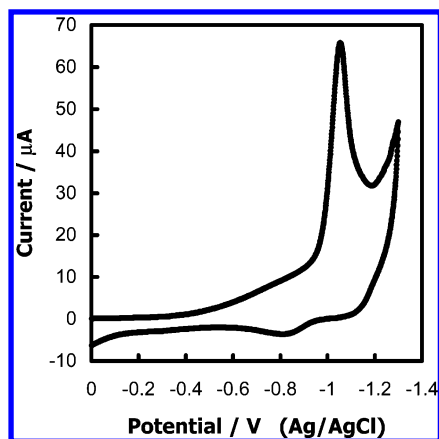


Figure 2. Cyclic voltammogram of $S(CH_2)_{11}OH$. The voltammetric scan rate is 0.1V/s.

defined by an elastomer O-ring^{22,23} (geometric area 0.66 cm²). A Pt coil and a Ag/AgCl/KCl_{sat} electrode were used as the auxiliary and reference electrodes, respectively. All measurements were made in 0.1 M KOH solutions at a scan rate of 0.1 V/s. The solutions were degassed with N₂ for 10 min prior to cycling.

Contact Angles. Sessile contact angles were measured using an FTA125 contact angle/surface tension instrument (First Ten Angstroms, Portsmouth, VA) on both sides of static drops. Before the characterization of the surfactant solutions, the contact angle of water was determined on each slide five times on different areas. The slide was then dried, and surfactant solution drops were applied. Measurements were recorded at 22 ± 2 °C.

Results and Analysis

Determination of Covalently Bound Surface Charge Density. Each ω -TMA molecule has exactly one positive charge. Hence, σ_c can be determined from eq 1. The surface mole fraction of ω -TMA molecules in the SAM, α , and the SAM density, Γ_{SAM} , are determined experimentally. Γ_{SAM} is measured by cyclic voltammetry. Figure 2 shows the cyclic voltammogram curve for a ω -OH monolayer on a Au (111) surface. The potential is scanned at a rate of 0.1 V/s from 0.0 V to -1.3 V. A sharp peak is observed at -1.06 V, which we assign to the reductive desorption of ω -OH on the basis of the similarity of this peak to results obtained for alkane thiols.^{23–26} The area under the peak, after compensating for the charging current, gives the charge associated with the reduction of ω -OH. If we assume that a single electron is required for the reduction of one ω -OH molecule, Γ_{SAM} ²⁷ is 3.4 ± 0.3 molecules/nm². We are unable to accurately determine the SAM densities of ω -TMA and mixed SAMs because the voltammograms are more complex. This complexity probably arises from the presence of highly-charged N⁺(CH₃)₃ groups.

For SAMs containing ω -TMA, we use XPS measurements to calculate the SAM density. These measurements are calibrated using the value of Γ_{SAM} obtained from cyclic voltammograms for the SAM containing only ω -OH. We assume that, on substrates with the same Au layer thicknesses, the ratio of the sulfur peak area S to the Au peak area Au (i.e., S/Au) is directly proportional to the density of thiolate molecules chemisorbed on Au. Therefore,

$$\Gamma_{SAM} = \frac{\Gamma_{SOH-only}}{(S/Au)_{SOH-only}} (S/Au) \quad (2)$$

TABLE 1: Normalized XPS Photopeak Area Ratios for SAM Films Prepared from Chloroform Solutions of HS(CH₂)₁₁N⁺(CH₃)₃Cl[−] and HS(CH₂)₁₁OH^a

X_N	N/S	S/Au
1	1.00 ± 0.06	0.053 ± 0.007
0.5	0.4 ± 0.1	0.06 ± 0.01
0.25	0.21 ± 0.06	0.065 ± 0.005
0	0	0.076 ± 0.009

^a X_N is the mole fraction of HS(CH₂)₁₁N⁺(CH₃)₃Cl[−] in 2 mM chloroform solutions.

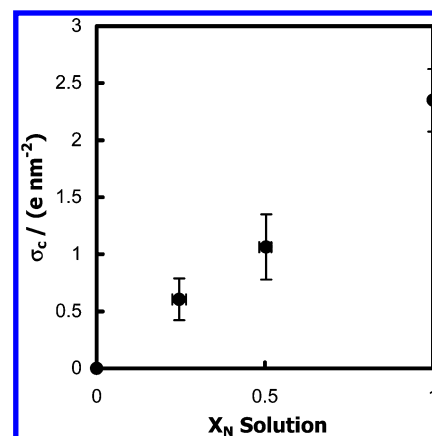


Figure 3. Surface charge density vs mole fraction of HS(CH₂)₁₁N⁺(CH₃)₃Cl[−] in solution. X_N is the mole fraction of HS(CH₂)₁₁N⁺(CH₃)₃Cl[−] in 2 mM chloroform solution.

The peak area ratios of S/Au for SAMs prepared from $H\omega$ -TMA and $H\omega$ -OH are given in Table 1.

The only parameter left to determine the surface charge density is the surface mole fraction of ω -TMA on SAMs, α . The value for α can be directly obtained from XPS measurements from the ratio of the areas of the nitrogen, N , and sulfur, S , peaks (N/S) and is shown in Table 1. Given Γ_{SAM} and α , the calculation of σ_c is trivial using eq 1.

The surface charge densities of SAMs prepared from $H\omega$ -TMA, $H\omega$ -OH, and their mixtures are plotted in Figure 3 as a function of the mole fraction of $H\omega$ -TMA in solution. As expected, when the mole fraction of $H\omega$ -TMA is increased in solution, σ_c increases. The linear relationship between the film density and solution composition supports our assumption that there are no clusters of ω -TMA and facilitates the interpolation to other solution compositions. For a mole fraction of 0.75 $H\omega$ -TMA, we interpolate the surface charge density to be 1.7 e/nm².

As expected, the presence of charged and bulky ω -groups on the surface reduces the SAM density. (See Figure 4.)

Adsorption Isotherms of SDS. We have employed SPR to measure the adsorption of SDS on SAMs. This procedure was pioneered by Sigal et al.²⁸ SPR is used to probe refractive index changes that occur within the immediate vicinity (~200 nm) of a sensor (gold) surface. Therefore, any physical phenomenon that alters the refractive index will elicit a response. In SPR, a monochromatic, p-polarized light excites the surface plasmons (SP) as well as being partially reflected off the gold film to an optical photodetector. The reflected light intensity is the analytical signal. A lower intensity of light reflected from the gold film indicates a higher degree of SP excitation. The maximum excitation of SP occurs at a specific angle, Θ , where the reflected light intensity has a minimum. The value of Θ depends on the refractive index of the adjacent medium.²⁹

SPR is sensitive both to the adsorbed surfactants and to the presence of molecules dissolved in the medium.³⁰ Here, we wish to obtain the surface excess of SDS, so we must subtract the

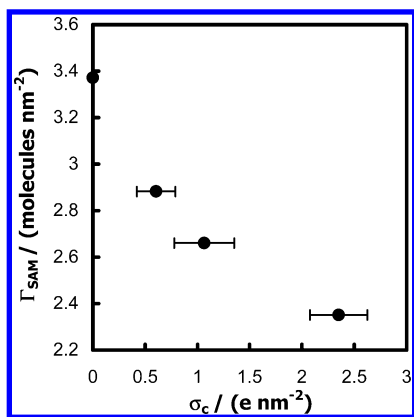


Figure 4. SAM density vs surface charge density. There is a systematic error of 0.3 molecules/nm² in the SAM density in all data points. The presence of ω -TMA decreases the density of the SAM.

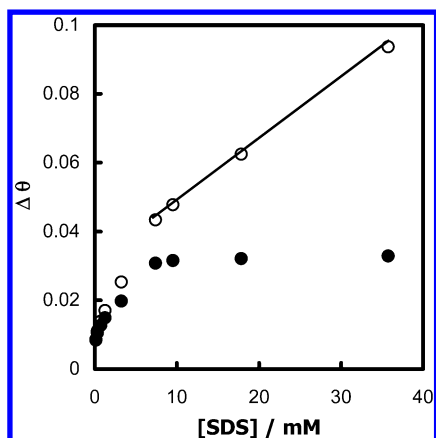


Figure 5. Change in angle of minimum reflected light intensity as a function of SDS concentration for a surface with $\sigma_c = 0.6$ e/nm². Open circles show the change in angle with respect to water. The straight line is fitted to the points above the cmc, where we assume that the surface excess is approximately constant. The filled circles are determined by subtracting the bulk contribution, which is obtained from the best-fit line.

contribution due to the bulk solution. In surfactant solutions the existence of a constant chemical potential, μ , region above the critical micelle concentration provides a convenient regime for calibrating the contribution from the bulk solution.

Figure 5 shows the change in angle, $\Delta\Theta$, with respect to water as a function of SDS concentration on surfaces with $\sigma_c = 0.6$ e/nm². When μ is constant, we assume that the adsorption is constant, and in support of this assumption we observe a linear relationship between $\Delta\Theta$ and c . The value of $\delta\Theta/\delta c$ is determined to be $0.0017 \pm 0.0001^\circ/\text{mM}$ from the slope of the line. Subtracting this bulk effect leaves only the angle change due to the surfactant adsorption on the surface, $\Delta\Theta_a$.²⁸

$$\Delta\Theta_a = \Delta\Theta - c \frac{\partial\Theta}{\partial c} \quad (3)$$

To obtain the amount of SDS adsorbed on self-assembled monolayers, the following equation is used^{31,32}

$$\Gamma = d \Delta n \frac{1}{\partial n / \partial c} \quad (4)$$

where d is the thickness of the adsorbed layer, $\delta n / \delta c$ is the refractive index increment of the surfactant, and Δn is the difference between the refractive index of the adsorbed SDS layer (1.45)^{28,30,33,34} and water (1.33).

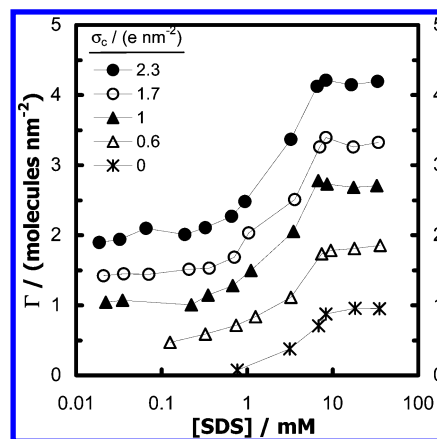


Figure 6. Adsorption of SDS to a series of SAMs of fixed surface charge, σ_c . Note that the error in σ_c is large (see Figure 3). The lines are guides to the eye.

The refractive index increment of the surfactant can be determined as follows:

$$\frac{\partial n}{\partial c} = \frac{\partial n}{\partial \Theta} \frac{\partial \Theta}{\partial c} \quad (5)$$

Here, $\delta\Theta/\delta n$ is an instrument constant (53°) and is supplied by the manufacturer of the SPR instrument. We have also carried out Fresnel calculations for a glass slide with a 40 nm gold layer on a sapphire prism. From these we find $\delta\Theta/\delta n = 53.6^\circ$.³⁵ Using eq 5, we find the refractive index increment of SDS to be $(3.2 \times \pm 0.2) \times 10^{-5} \text{ mM}^{-1}$, which is within 3% of previously reported values.^{28,36}

The thickness of the layer is determined using eq 6:

$$d = \Delta\Theta_a \frac{\partial d}{\partial \Theta} \quad (6)$$

The value of $\delta\Theta/\delta d = 0.04^\circ/\text{nm}$ is obtained from a Fresnel calculation.³⁵

In summary, the surface excess is experimentally obtained as follows:

$$\Gamma = \Delta\Theta_a \frac{\partial d}{\partial \Theta} \Delta n \frac{\partial \Theta}{\partial n} \frac{\partial c}{\partial \Theta} \quad (7)$$

Figure 6 shows the adsorption of SDS from aqueous solution to SAMs of various surface charge densities. Note that the raw data do not allow us to distinguish DS[−] from SDS. There is little adsorption onto the uncharged ω -OH SAM up to about 2 mM SDS. The shape of the adsorption isotherms for charged surfaces is independent of the surface charge density: all show two plateau regions. The first-plateau region ends at about 0.3 mM (cmc/25). On the 2.3 e/nm² surface, the area per molecule in the first plateau is about 0.5 nm², which is slightly larger than the area per molecule at the air–SDS solution interface just below the cmc ($0.41 \pm 0.06 \text{ nm}^2$).³⁷ For all surfaces, there is a plateau above 8 mM (the cmc). Above this concentration, the chemical potential is only a weak function of concentration.

Figure 7 shows the adsorbed amount of SDS (from Figure 6) as a function of surface charge density. All data points are the average values for the adsorbed amount of SDS in the respective region. The filled circles represent the SDS adsorption in the first-plateau regions. The data points fall on a line with a slope of one, showing that the amount of adsorbed SDS per unit area in the first plateaux corresponds to the surface charge density. DS[−] is the most common counterion, and every positive surface site has an attached DS[−] counterion. But, there appears

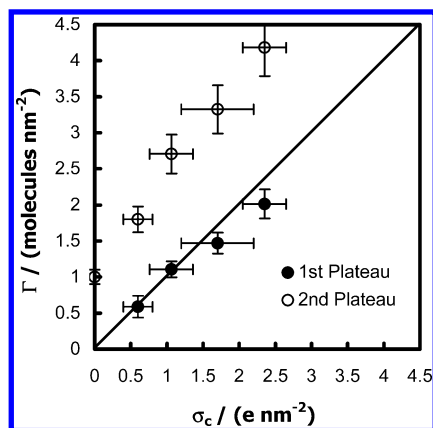


Figure 7. Adsorbed density of SDS vs surface charge density. In the first-plateau region, approximately one surfactant molecule adsorbs for each covalently bound surface charge.

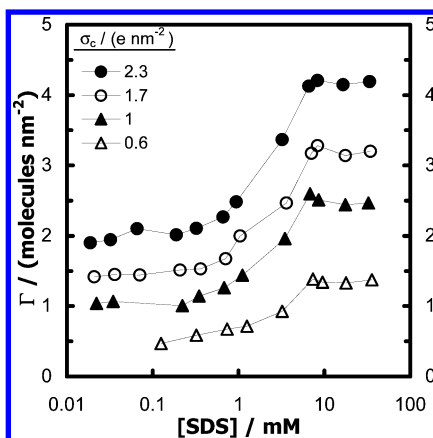


Figure 8. Adsorption isotherms of SDS. The amount of SDS adsorbed per OH group at $\sigma_c = 0$ e/nm² surfaces has been subtracted from each adsorption isotherm.

to be no additional SDS adsorption, even when the density of surface charge is high, that is, the high density of alkyl chains does not promote adsorption of a superequivalent amount of DS[−] or SDS. The unfilled circles represent the surface excess of SDS in the second-plateau regions. Adsorption in the second plateaux increases linearly with surface charge density. This indicates that there is no abrupt change in SDS adsorption as a function of surface charge density. Again, there is no critical charge density that produces a superequivalent adsorption of DS[−] or SDS.

There is some adsorption on surfaces with $\sigma_c = 0$ e/nm² (ω -OH only SAMs) at concentrations greater than 0.8 mM. This adsorption was also observed in ref 30. To examine the effect of the change in charge on SDS adsorption, we have plotted the same data in Figure 8 as in Figure 6 after subtraction of an estimate of the contribution due to adsorption from the ω -OH groups. The adsorption of SDS to ω -OH groups is approximated as the product of the amount of SDS adsorbed per OH group to the ω -OH-only film and the density of OH groups. This is only a rough estimate, as it is reasonable to expect interaction of the surfactant with more than one surface group. The same procedure has been repeated for all surfaces except for $\sigma_c = 2.3$ e/nm², which does not have any ω -OH. This adjustment has no effect on the first-plateau regions of the adsorption isotherms of surfaces with $\sigma_c = 1.7$ and 1.0 e/nm².

Figure 9 shows the ratio between the adsorbed amount in the first- and second-plateau regions. The filled and unfilled circles represent the data used from Figure 8 and Figure 6, respectively. This graph shows that SDS adsorption in the

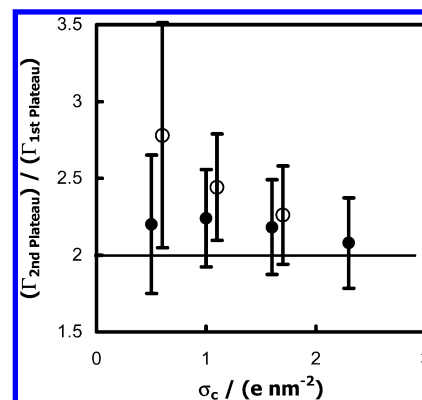


Figure 9. Comparison of SDS adsorption in the first- and second-plateau regions. The filled and unfilled circles represent the ratio of the adsorbed amount of SDS in the second- and first-plateau regions calculated from Figure 8 and Figure 6, respectively.

second plateaux is approximately 2–2.8 times the adsorption in the first plateaux. If the second-plateau data are adjusted to account for adsorption to the ω -OH groups, the adsorption in the second plateaux is about twice the adsorption in the first plateaux, independent of surface charge.

Table 2 gives contact angles of water and SDS solutions on SAMs. The data show that we are able to vary the surface charge density from 0 to 2.3 e/nm² with only a small variability in the wettability by water (36–48°). The surfactant concentrations shown in bold are 0.32 mM and 16 mM. The 0.32 mM concentration is the end of the first plateau and the 16 mM concentration is in the second plateau. The contact angle has a maximum at 0.32 mM, and from there it decreases for all surfaces. This increase in wettability at concentrations above the first plateau is consistent with the adsorption of additional surfactant with their heads toward the solution. Above the cmc, the contact angle has a large hysteresis, which is consistent with facile adsorption and desorption of at least part of the adsorbed surfactant. Therefore, the contact angle data is consistent with a first layer of surfactant with tails oriented toward the solution in the first plateau and a second layer of surfactant with heads oriented toward the solution in the second plateau.

Figure 10 shows the *desorption* of SDS from SAMs with different surface charge densities into pure water. The variation in bulk concentration during this experiment affects the analysis of these data. When 16 mM SDS is present in the cell (approximately the first 100 s), the adsorbed amount of SDS is calculated as described previously. When there is only water flowing through the cell (approximately after 150 s), there is no need to make a correction for SDS in the bulk solution. Therefore, eq 7 is used by replacing $\Delta\Theta_a$ with $\Delta\Theta$. During the switch from 16 mM SDS to water, we should subtract a contribution due to the changing of the SDS concentration *near* the interface (the bulk effect in eq 3), but the time dependence of the change in concentration near the surface is not known. However, this error in surface excess does not have a significant effect on our current analysis because the initial desorption is almost vertical on the time scale of our results.

The desorption isotherms show two regions for charged surfaces: a fast rate of desorption followed by a slow rate of desorption. Similar fast desorption rates were obtained by Sigal et al.²⁸ for the desorption of SDS from hexadecanethiol SAMs. In their study, there is only a single layer of SDS bound to the hydrophobic SAM. The onset of the slow desorption region corresponds approximately to the surface charge density of the surfaces. (See Figure 11.) For example, in the films with no

TABLE 2: Contact Angles, θ , of Aqueous SDS Solutions on SAMs with Different Surface Charge Densities^{a,b}

concentration (mM)	θ ($\sigma_c = 0.6 \text{ e/nm}^2$)	θ ($\sigma_c = 1.0 \text{ e/nm}^2$)	θ ($\sigma_c = 1.7 \text{ e/nm}^2$)	θ ($\sigma_c = 2.3 \text{ e/nm}^2$)
0	44 ± 9	48 ± 7	36 ± 4	38 ± 10
0.16	65 ± 5	65 ± 8	51 ± 2	66 ± 3
0.32	65 ± 4	64 ± 3	57 ± 3	70 ± 1
4	50 ± 3	43 ± 5		61 ± 1
16	32 ± 6	49 ± 7	43 ± 5	45 ± 3
16 advancing	44 ± 6	70 ± 7	61 ± 6	49 ± 4
16 receding	26 ± 4	37 ± 6	20 ± 5	15 ± 3

^a The contact angle of water on the ω -OH surface is $36 \pm 4^\circ$. ^b The bold surfactant concentrations, 0.32 mM and 16 mM, are the end of the first plateau and in the second plateau, respectively.

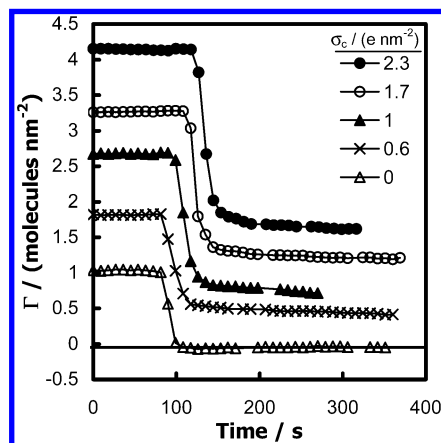


Figure 10. Desorption isotherms of SDS from SAMs with different surface charge densities. The SDS concentration is 16 mM ($2 \times \text{cmc}$) at time zero. The time at which the solution was switched from $2 \times \text{cmc}$ to water was shifted arbitrarily to allow a clear view of all the curves.

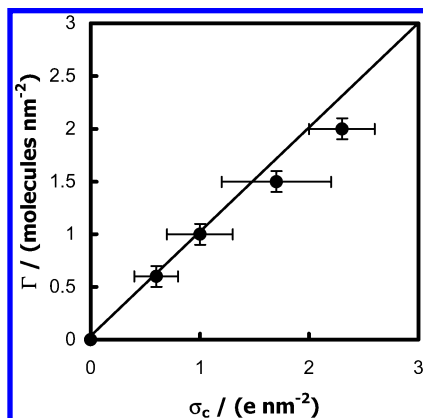


Figure 11. The surface excess remaining ~ 30 s after the bathing solution was switched from $2 \times \text{cmc}$ to pure water.

surface charges (ω -OH SAMs) the surface excess drops to zero within a few seconds. This data is consistent with two adsorption sites. There is a rapid loss of nonelectrostatically bound surfactant (as for ref 28) followed by a slow loss of electrostatically bound surfactant. In other work we³⁸ have shown that desorption of the electrostatically bound surfactant is accelerated by the presence of additional electrolyte. This suggests that desorption of charged species in water is hindered by the production of an opposite potential on the surface. This potential is reduced through adsorption of counterions from the electrolyte.

Structure of Adsorbed SDS Aggregates. We have employed AFM to investigate the surface homogeneity of SAMs³⁹ and the structure of adsorbed surfactant aggregates⁴⁰ on SAMs.⁴¹

In water, the force between the negatively charged AFM tip and the positively charged SAMs is attractive, as expected. The

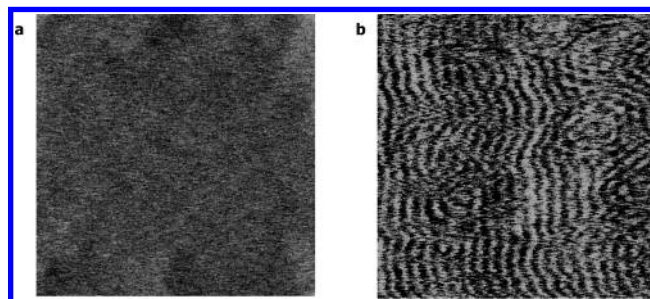


Figure 12. (a) 150-nm AFM image of the interface between a SAM with $\sigma_c = 2.3 \text{ e/nm}^2$ and 16 mM SDS solution. (b) 150-nm AFM image of the interface between SAM with $\sigma_c = 2.3 \text{ e/nm}^2$ and 16 mM SDS solution with 0.1 M NaCl. The period of the cylindrical micelles is ~ 7 nm.

images are featureless in water: there are no holes or aggregates and the root mean square roughness is $0.12 \pm 0.05 \text{ nm}$ for an area of $200 \text{ nm} \times 200 \text{ nm}$. These observations support the homogeneity of SAMs formed from ω -TMA, ω -OH, and mixtures of the two on gold.

Figure 12a shows the AFM image of the interface between the SAM with $\sigma_c = 2.3 \text{ e/nm}^2$ and the 16 mM ($2 \times \text{cmc}$) SDS solution. No features on the surface are resolved by our imaging. This is consistent with the formation of a bilayer on the surface, although it is possible that imaging with the tip does disrupt surface aggregates that are there in the absence of the tip. That our imaging technique does have the ability to resolve features is demonstrated through the addition of salt. In Figure 12b we observe cylindrical micelles in 16 mM SDS and 0.1 M NaCl. The sum of the cylinder diameter and the intermicellar separation is $7.0 \pm 0.3 \text{ nm}$. The cylinders are mainly parallel to each other. We observe a similar behavior for surfaces with $\sigma_c = 1.7 \text{ e/nm}^2$. In contrast, in bulk the addition of salt usually causes aggregates to adopt a smaller curvature.⁴² The formation of discrete structures on the surface in the presence of the salt suggests that charge regulation is important for the formation of discrete structures on surfaces.

The images are featureless on pure ω -OH surfaces in the presence of 16 mM SDS. The force curves change from being slightly attractive in water to being repulsive in SDS solution, with no jump-in. The repulsive force is expected for the interaction between a charged and a neutral surface. AFM images of surfaces with $\sigma_c = 0.6 \text{ e/nm}^2$ and $\sigma_c = 1.0 \text{ e/nm}^2$ do not have any distinct features in 16 mM SDS solutions nor in 0.1 M NaCl and 16 mM SDS solutions. On some occasions we have observed some structures that are 7 nm in size (not shown), but the structure is not force-sensitive. Resolution of surfactant aggregates is always force-sensitive,^{40b} so we do not attribute these structures to adsorbed material.

The position of a mechanical instability of the AFM tip on approach to an adsorbed surfactant film is sometimes used to indicate the thickness of the film.⁴³ The instability (jump-in)

TABLE 3: Tip–SAM Separation for the Mechanical Instability in AFM Force Measurements in $2 \times \text{cmc}$ SDS Solution

σ_c (e/nm^2)	separation (nm)
0	no instability
0.6	0.8
1.0	2.7
2.3	3.4

occurs when the spring constant is smaller in magnitude than the gradient of the surface force. This jump-in is not simply related to the thickness of the film; however, we will use it as an indicator of a trend in thickness. Table 3 shows that at $2 \times \text{cmc}$ there is a systematic increase in jump-in distance with an increase in surface charge density. This is consistent with an increase in surfactant film thickness with an increase in surface charge density.

Discussion

Mechanism of SDS Adsorption on Fixed-Charge Surfaces. Interpretation of adsorption isotherms gives useful information about the mechanism of SDS adsorption on fixed-charge surfaces in the absence of salt. In the first-plateau region in Figure 6, the 1:1 relationship between the surfactant adsorption and surface charge density shows that surface charge governs the surfactant adsorption. These experimental results agree well with the theoretical calculations of Böhmer and Koopal⁴⁴ for adsorption of ionic surfactants on constant charge surfaces. Their calculations have also shown that there is a plateau region at low concentrations where the surfactant adsorption per area equals the surface charge density. Experiments on (charge-regulating) silica surfaces show that there is an adsorption plateau in which the surface excess of the cationic surfactant is approximately equal to the surface charge density.⁷

At higher SDS concentrations, there is an increase in the adsorbed amount and contact angle measurements suggest that the headgroups are directed toward the solution. There is approximately twice the level of adsorption at the second-plateau region compared to the first-plateau region (Figure 9) for all values of σ_c . All these data are consistent with the formation of a bilayer of surfactant molecules for all surface charge densities but with a thickness that increases with the surface charge density.

It is interesting that the adsorbed amount in the first plateau is always about the same as the surface charge. There does not appear to be a critical surface density of surfactant that leads to adsorption of surfactant in excess of one molecule per charged site. Therefore, the phenomenon of a hemimicelle concentration does not appear to exist for the conditions of our experiment, where there is no charge regulation. This is contrary to a recent review by Atkin et al.⁵ where they suggest that a certain density of surfactant is required to cause aggregation: we can vary the average density of surfactant over a large range without initiating hemimicelle formation.

In addition, the second plateau is always about twice the level of the first plateau. The first layer does not appear to be a nucleation site for a much larger structure. A reasonable model for adsorption after the first plateau is a repeat of the structure in the first plateau but with the opposite orientation of the molecules.

There is no a priori reason that the effects of compositional changes in the SAM should produce additive changes in adsorption. However, noting that the adsorption in the first plateau scaled directly with the density of charged groups, we

sought a simple relationship for adsorption in the second layer. If we subtract an estimate for adsorption due to the ω -OH groups, we find that adsorption due to the ω -TMA groups at and above the cmc is about double the adsorption due to the ω -TMA groups in the first plateau. If this subtraction is performed, the curves for all charge densities follow a simple form: a plateau with a one-to-one relationship between adsorption and surface charge followed by a plateau with a two-to-one relationship between adsorption and surface charge at and above the cmc.

Morphology of Surfactants on Fixed-Charge Surfaces. We did not observe any discrete surfactant aggregates on the SAMs in $2 \times \text{cmc}$ SDS. It is very interesting that no micelles are detected at the lower surface charge densities, where the magnitude of the surface charge density is comparable to that of silica. In contrast, surface micelles of tetradecyltrimethylammonium bromide⁴⁵ and hexadecyltrimethylammonium bromide¹⁵ have been imaged on silica. There is enough SDS adsorption to form micelles at $2 \times \text{cmc}$ on the SAMs (Figure 6) but the surfactant forms a homogeneous film (as observed by AFM) rather than discrete micelles. We hypothesize that the inability to form discrete surface aggregates of SDS surfactants is due to the lack of clusters of counter charges on the solid. The clustering of charges is normally made possible by charge regulation.

On natural surfaces such as silica and alumina the surface charges are not fixed because the surfaces contain dissociable groups that respond to the surface electrical potential (charge regulation).^{1,5,7} Charge regulation on these surfaces has two effects: it can change the average surface charge density and it can change the distribution of charges on the surface. Considering now an anionic surfactant, when one molecule of surfactant adsorbs with its charge near the solid, a new positive surface charge can be created by association or dissociation of a surface ion. The net effect is an increase in the surface charge density but not an equimolar increase in the outer surface charge. The important point is that on a chemically homogeneous surface, the most favorable site for the creation of the new surface charge is in the immediate vicinity of the adsorbed surfactant, because the anionic surfactant has decreased the *local* electrical potential. This concept has also been discussed by Atkin et al. in a recent review.⁵ For cationic surfactant adsorbed to silica, they describe how surfactant adsorption will increase the acidity of nearby silanol groups thereby creating new negatively charged sites near the site of the originally adsorbed surfactant. In contrast, Goloub and Koopal⁹ suggest that new charges are *not* created in the vicinity of adsorption sites on *silica* but that new charges are created in the vicinity of adsorption sites on *rutile*.

Surface micellization is facilitated by the lateral mobility of surface ions because continued surfactant adsorption can occur without locally building up a charge that is unfavorable to the surfactant adsorption and without the entropic cost of pulling counterions from the solution. Surface charge regulation that leads to the formation of counterions for the surfactant that are remote from the initial adsorbed surfactant molecule or the creation of more charges (through SAM techniques) that are remote from each other does not aid surface micellization by as much, even though both processes lead to greater average surface charge. Thus, average surface charge density (or potential) is not a sufficient parameter to predict surface micellization.

On a homogeneous SAM surface, prepared from fixed charged groups, we expect random or evenly distributed surface charges and therefore no inducement to form a surface micelle.

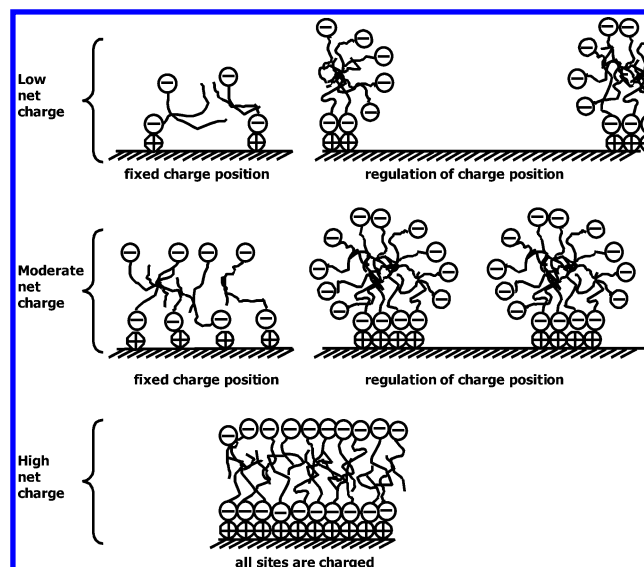


Figure 13. Effect of surface charge distribution on surfactant adsorption above the cmc. The situation in the top right would only occur in the unusual case where there is a fixed number of mobile surface charges (e.g., on a short-chained or high-temperature SAM). More commonly, the surface groups will have a finite pK, and effective mobility is attained by association at one point and dissociation at another point. One would always expect the net charge of this type of surface to increase in magnitude because of adsorption of oppositely charged surfactant.

The very different adsorption behavior on charge-regulating surfaces and on nonregulating surfaces supports the hypothesis that clusters of counter charges are important to promote surface micellization. This can be achieved through lateral mobility of surface sites or through surface charge regulation on a surface with a high density of dissociable sites. This is shown schematically in Figure 13.

By experiment, we find that when the density of fixed charges is made very high the surfactant adsorbs to form a continuous layer on the surface, despite the fact that SDS forms spherical micelles in solution. Again, there are no discrete surface micelles in the absence of surface charge regulation.

Although the covalently bound surface charge cannot regulate, micelles are formed in the presence of NaCl, presumably because Cl^- competes with DS^- for quaternary ammonium sites and reduces the number of available positive sites. The mobility of the Cl^- ions allows the clustering of available cationic surface sites and, therefore, allows the formation of micelles. The extra Na^+ can also bind to the DS^- headgroups, reducing the interaction between the DS^- and the surface charges. This relaxes the templating effect of the fixed, planar arrangement of surface charges on the adsorbed micelle shape. A similar phenomenon was observed for C_{16}TABr on mica: a flat layer of C_{16}TABr formed on mica in the absence of salt and discrete micelles were formed in the presence of salt.^{4,46}

The absence of adsorbed micelles of SDS on fixed-charge surfaces leads us to conclude that *lateral mobility* of ions other than the surfactant is very important for forming surface micelles of charged surfactants. In this paragraph we consider exceptions to this idea. First, we predict that surface micellization of charged surfactants will be found for a surface that contains preexisting micellar-size clusters of counter charges. Second, the molecular shape of certain surfactants might prevent those surfactants from forming flat sheets of adsorbate even on fixed-charge surfaces. A prediction of this effect could be based either on the packing parameter model⁴² or on the experimental absence of lamellar structures anywhere in the phase diagram.

For example, ionic surfactants that have a very large van der Waals cross section through the headgroup or fixed spacing between headgroups (e.g., Gemini surfactants) may not be able to form lamellar structures on surfaces. Perhaps the closest examples of a fixed-charge surface is mica, which however does undergo charge regulation due to the adsorption of protons.^{47,48} Experiments show that surfactants with bulky headgroups (e.g., triethylammonium and tripropylammonium)⁴⁹ and Gemini surfactants^{50,51} form discrete micelles on mica. The arrangement of charge on the solid surface should cause the largest differences between solution and surface micelle shapes when there is a large difference between the headgroup area in a bulk micelle (the effective headgroup area)⁴² and the headgroup area calculated from van der Waals radii.

Conclusions

We have prepared surfaces with known and controlled surface charge densities, σ_c , in the range of $0\text{--}2\text{ e/nm}^2$ from SAMs prepared from $\text{HS}(\text{CH}_2)_{11}\text{OH}$ and $\text{HS}(\text{CH}_2)_{11}\text{N}^+(\text{CH}_3)_3\text{Cl}^-$ on gold. The adsorption isotherm of SDS on the charged SAM surfaces in the absence of additional salt shows two plateau regions. The first plateau ends at about $\text{cmc}/25$. For each surface charge density, the density of surfactant adsorbed in the first plateau is approximately equal to the surface charge density, so clearly σ_c governs the surfactant adsorption. There is a second plateau above the cmc (where the chemical potential rises very slowly). Above the cmc, the adsorption is about two times the adsorption in the first plateau, for a range of surface charge densities. The change in wettability suggests that the headgroups of the additional surfactant face toward the aqueous phase. Surprisingly, there is no critical value of σ_c that leads to a disproportionate rise in surfactant adsorption, and the *shape* of the isotherm is almost independent of σ_c .

Micelles are not observed using AFM on any of the surfaces in the absence of salt. Our results show that when the surface charge is homogeneously distributed and fixed and the surfactant is almost the only counterion available, a homogeneous distribution of the surfactant across the surface is at a lower energy than an inhomogeneous distribution. The addition of mobile counterions to the surface charge (other than the surfactant) allows the introduction of lateral inhomogeneity in the surfactant adsorption. This leads us to hypothesize that, for ionic surfactants, a lateral redistribution of surface charge to produce a heterogeneous surface charge (a form of charge regulation) is important for forming the heterogeneous surfactant layers known as surface micelles. This effect should be particularly important for surfactants in which the optimal area occupied by the surfactant headgroup in solution is a function of solution conditions. Because lateral charge regulation is an important factor in allowing the formation of surface micelles, it is also an important factor in determining the shape of the adsorption isotherm for ionic surfactants.

Acknowledgment. We thank Mark Anderson for the use of his equipment and for his advice regarding the reduction and cyclic voltammetry experiments, Ray Dessy for help and advice with the use of the SPR and for providing the optical simulation program, Frank Cromer for help with the XPS experiments, and Reicherdt Incorporated for the complementary use of their β -SPR instrument. This material is based upon work supported by the National Science Foundation under Grant No. CHE-0203987 and the Petroleum Research Fund under Grant No. 36327-AC5.

References and Notes

- (1) Somasundaran, P.; Fuerstenau, D. W. *J. Phys. Chem.* **1966**, *70*, 90–96.
- (2) Bohmer, M. R.; Koopal, L. K. *Langmuir* **1992**, *3*, 2649–2659.
- (3) Fleming, B. D.; Biggs, S.; Wanless, E. J. *J. Phys. Chem. B* **2001**, *105*, 9537–9540.
- (4) Lamont, R. E.; Ducker, W. A. *J. Am. Chem. Soc.* **1998**, *120*, 7602–7607.
- (5) Atkin, R.; Craig, V. S. J.; Wanless, E. J.; Biggs, S. *Adv. Colloid Interface Sci.* **2003**, *103*, 219–304.
- (6) Yates, D. E.; Levine, S.; Healy, T. W. *J. Chem. Soc., Faraday Trans. 1* **1974**, *70*, 1807–1818.
- (7) Goloub, T. P.; Koopal, L. K.; Bisterbosch, B. H.; Sidorova, M. P. *Langmuir* **1996**, *12*, 3188–3194.
- (8) Chandar, P.; Somasundaran, P.; Turro, N. J. *J. Colloid Interface Sci.* **1987**, *117*, 31–46.
- (9) Goloub, T. P.; Koopal, L. K. *Langmuir* **1997**, *13*, 673–681.
- (10) Bisterbosch, B. H. *J. Colloid Interface Sci.* **1974**, *47*, 186–98.
- (11) Gaudin, A. M.; Fuerstenau, D. W. *Trans. AIME* **1955**, *202*, 958–962.
- (12) Somasundaran, P.; Healy, W. T.; Fuerstenau, D. W. *J. Phys. Chem.* **1964**, *68*, 3562–3566.
- (13) (a) Nuzzo, R. G.; Allara, D. L. *J. Am. Chem. Soc.* **1983**, *105*, 4481–4483. (b) Porter, M. D.; Bright, T. B.; Allara, D. L.; Chidsey, C. E. D. *J. Am. Chem. Soc.* **1987**, *109*, 3559–3568. (c) Bain, C. D.; Troughton, E. B.; Tao, Y.-T.; Evall, J.; Whitesides, G. M.; Nuzzo, R. G. *J. Am. Chem. Soc.* **1989**, *111*, 321–335.
- (14) Nuzzo, R. G.; Dubois, L. H.; Allara, D. L. *J. Am. Chem. Soc.* **1990**, *112*, 558–569.
- (15) Subramanian, V.; Ducker, W. A. *Langmuir* **2000**, *16*, 4447–4454.
- (16) Ninham, B. W.; Yaminsky, V. *Langmuir* **1997**, *13*, 2097–2108.
- (17) Tien, J.; Terfort, A.; Whitesides, G. M. *Langmuir* **1997**, *13*, 5349–5355.
- (18) Schmidt, L. D. *CRC Crit. Rev. Solid State Mater. Sci.* **1978**, *7*, 129–141.
- (19) Hsu, T.; Cowley, J. M. *Ultramicroscopy* **1983**, *11*, 239–250.
- (20) Honbo, H.; Sugawara, S.; Itaya, K. *Anal. Chem.* **1990**, *62*, 2424–2429.
- (21) Synder, S. R. *J. Electrochem. Soc.* **1992**, *139*, 5C–8C.
- (22) Rowe, G. K.; Creager, S. E. *Anal. Chim. Acta* **1991**, *246*, 233–239.
- (23) Widrig, C. A.; Chung, C.; Porter, M. D. *J. Electroanal. Chem.* **1991**, *310*, 335–359.
- (24) Zhong, C.; Porter, M. D. *J. Electroanal. Chem.* **1997**, *425*, 147–153.
- (25) Yang, D. F.; Wilde, C. P.; Morin, M. *Langmuir* **1996**, *12*, 6570–6577.
- (26) Hobara, D.; Ota, M.; Imabayashi, S.; Niki, K.; Kakiuchi, T. *J. Electroanal. Chem.* **1998**, *444*, 113–119.
- (27) Walczak, M. M.; Popenoe, D. D.; Deinhammer, R. S.; Lamp, D. B.; Chung, C.; Porter, M. D. *Langmuir* **1991**, *7*, 2687–2693.
- (28) Sigal, G. B.; Mrksich, M.; Whitesides, G. M. *Langmuir* **1997**, *13*, 2749–2755.
- (29) For a review, see: Earp, R. L.; Dessy, R. E. In *Commercial Biosensors: Applications to Clinical, Bioprocess, and Environmental Samples*; Ramsey, G., Ed.; Wiley: New York, 1998; p 99.
- (30) Sigal, G. B.; Mrksich, M.; Whitesides, G. M. *J. Am. Chem. Soc.* **1998**, *120*, 3464–3473.
- (31) de Feijter, J. A.; Benjamins, J.; Veer, F. A. *Biopolymers* **1978**, *17*, 1759–1772.
- (32) Schaaf, P.; Déjardin, P.; Schmitt, A. *Langmuir* **1987**, *3*, 1131–1135.
- (33) Kavanagh, R. J.; Iu, K. K.; Thomas, J. K. *Langmuir* **1992**, *8*, 3008–3013.
- (34) Tiberg, F.; Ederth, T. *J. Phys. Chem. B* **2000**, *104*, 9689–9695.
- (35) The simulation program is provided by Professor Raymond Dessy, Chemistry Department, Virginia Tech, Blacksburg, VA.
- (36) Nakagaki, M.; Shimabayashi, S. *Nippon Kagaku Kaishi* **1976**, *9*, 1353–1357.
- (37) The area per molecule of SDS at the air–SDS solution interface given in the text is the average and the standard deviation of the literature values: (a) Cook, M. A.; Talbot, E. L. *J. Phys. Chem.* **1952**, *56*, 412–416. (b) Davies, J. T. *J. Colloid Sci.* **1956**, *11*, 377–390. (c) Wilson, A.; Epstein, M. B.; Ross, J. *J. Colloid Interface Sci.* **1957**, *12*, 345–355. (d) Tajima, K.; Muramatsu, M.; Sasaki, T. *Bull. Chem. Soc. Jpn.* **1970**, *43*, 1991–1998. (e) Hines, J. D. *J. Colloid Interface Sci.* **1996**, *180*, 488–492.
- (38) Clark, S. C.; Ducker, W. A. *J. Phys. Chem. B* **2003**, *107*, 9011–9021.
- (39) (a) Appelhans, D.; Ferse, D.; Adler, H.-J. P.; Plieth, W.; Fikus, A.; Grundke, K.; Schmitt, F.-J.; Bayer, T.; Adolph, B. *Colloids Surf., A* **2000**, *161*, 203–212. (b) Shon, Y.-S.; Lee, S.; Perry, S. S.; Lee, T. R. *J. Am. Chem. Soc.* **2000**, *122*, 1278–1281. (c) Abdelghani, A. *Mater. Lett.* **2001**, *50*, 73–77.
- (40) For reviews see: (a) Manne, S. *Prog. Colloid. Polym. Sci.* **1997**, *103*, 226–233. (b) Ducker, W. A. In *Adsorption and Aggregation of Surfactants in Solution*; Mittal, K. L., Shah, D., Eds.; Marcel Dekker: New York, 2003; p 219.
- (41) Grant, L. M.; Ederth, T.; Tiberg, F. *Langmuir* **2000**, *16*, 2285–2291.
- (42) Israelachvili, J. N. *Intermolecular and Surface Forces*, 2nd ed.; Academic Press: San Diego, CA, 1991; Chapter 17.
- (43) Wanless, E. J.; Ducker, W. J. *J. Phys. Chem.* **1996**, *100*, 3207–3214.
- (44) Böhrer, M. R.; Koopal, L. K. *Langmuir* **1992**, *8*, 1594–1602.
- (45) Manne, S.; Gaub, H. E. *Science* **1995**, *270*, 1480–1482.
- (46) Ducker, W. A.; Wanless, E. J. *Langmuir* **1999**, *15*, 160–168.
- (47) Pashley, R. M. *J. Colloid Interface Sci.* **1981**, *83*, 531–546.
- (48) Pashley, R. M. *J. Colloid Interface Sci.* **1981**, *80*, 153–162.
- (49) Patrick, H. N.; Warr, G. G.; Manne, S.; Aksay, I. A. *Langmuir* **1999**, *15*, 1685–1692.
- (50) Manne, S.; Schaffer, T. E.; Huo, Q.; Hansma, P. K.; Morse, D. E.; Stucky, G. D.; Aksay, I. A. *Langmuir* **1997**, *13*, 6382–6387.
- (51) Fielden, M. L.; Claesson, P. M.; Verrall, R. E. *Langmuir* **1999**, *15*, 3924–3934.